BABAR-PUB-05/040
SLAC-PUB-11385
hep-ex/0508012

Search for Lepton Flavor Violation in the Decay $\tau^\pm \to e^\pm\gamma$

B. Aubert,[1] R. Barate,[1] D. Boutigny,[1] F. Couderc,[1] Y. Karyotakis,[1] J. P. Lees,[1] V. Poireau,[1] V. Tisserand,[1] A. Zghiche,[1] E. Grauges,[2] A. Palano,[3] M. Pappagallo,[3] A. Pompili,[3] J. C. Chen,[4] N. D. Qi,[4] G. Rong,[4] P. Wang,[4] Y. S. Zhu,[4] G. Eigen,[5] I. Ofte,[5] B. Stugu,[5] G. S. Abrams,[6] M. Battaglia,[6] A. B. Breon,[6] D. N. Brown,[6] J. Button-Shafer,[6] R. N. Cahn,[6] E. Charles,[6] C. T. Day,[6] M. S. Gill,[6] A. V. Gritsan,[6] Y. Groysman,[6] R. G. Jacobsen,[6] R. W. Kadel,[6] J. Kadyk,[6] L. T. Kerth,[6] Yu. G. Kolomensky,[6] G. Kukartsev,[6] G. Lynch,[6] L. M. Mir,[6] P. J. Oddone,[6] T. J. Orimoto,[6] M. Pripstein,[6] N. A. Roe,[6] M. T. Ronan,[6] W. A. Wenzel,[6] M. Barrett,[7] K. E. Ford,[7] T. J. Harrison,[7] A. J. Hart,[7] C. M. Hawkes,[7] S. E. Morgan,[7] A. T. Watson,[7] M. Fritsch,[8] K. Goetzen,[8] T. Held,[8] H. Koch,[8] B. Lewandowski,[8] M. Pelizaeus,[8] K. Peters,[8] T. Schroeder,[8] M. Steinke,[8] J. T. Boyd,[9] J. P. Burke,[9] N. Chevalier,[9] W. N. Cottingham,[9] T. Cuhadar-Donszelmann,[10] B. G. Fulsom,[10] C. Hearty,[10] N. S. Knecht,[10] T. S. Mattison,[10] J. A. McKenna,[10] A. Khan,[11] P. Kyberd,[11] M. Saleem,[11] L. Teodorescu,[11] A. E. Blinov,[12] V. E. Blinov,[12] A. D. Bukin,[12] V. P. Druzhinin,[12] V. B. Golubev,[12] E. A. Kravchenko,[12] A. P. Onuchin,[12] S. I. Serednyakov,[12] Yu. I. Skovpen,[12] E. P. Solodov,[12] A. N. Yushkov,[12] D. Best,[13] M. Bondioli,[13] M. Bruinsma,[13] M. Chao,[13] S. Curry,[13] I. Eschrich,[13] D. Kirkby,[13] A. J. Lankford,[13] P. Lund,[13] M. Mandelkern,[13] R. K. Mommsen,[13] W. Roethel,[13] D. P. Stoker,[13] C. Buchanan,[14] B. L. Hartfiel,[14] A. J. R. Weinstein,[14] S. D. Foulkes,[15] J. W. Gary,[15] O. Long,[15] B. C. Shen,[15] K. Wang,[15] L. Zhang,[15] D. del Re,[16] H. K. Hadavand,[16] E. J. Hill,[16] D. B. MacFarlane,[16] H. P. Paar,[16] S. Rahatlou,[16] V. Sharma,[16] J. W. Berryhill,[17] C. Campagnari,[17] A. Cunha,[17] B. Dahmes,[17] T. M. Hong,[17] M. A. Mazur,[17] J. D. Richman,[17] W. Verkerke,[17] T. W. Beck,[18] A. M. Eisner,[18] C. J. Flacco,[18] C. A. Heusch,[18] J. Kroseberg,[18] W. S. Lockman,[18] G. Nesom,[18] T. Schalk,[18] B. A. Schumm,[18] A. Seiden,[18] P. Spradlin,[18] D. C. Williams,[18] M. G. Wilson,[18] J. Albert,[19] E. Chen,[19] G. P. Dubois-Felsmann,[19] A. Dvoretskii,[19] D. G. Hitlin,[19] J. S. Minamora,[19] I. Narsky,[19] T. Piatenko,[19] F. C. Porter,[19] A. Ryd,[19] A. Samuel,[19] R. Andreassen,[20] G. Mancinelli,[20] B. T. Meadows,[20] M. D. Sokoloff,[20] F. Blanc,[21] P. Bloom,[21] S. Chen,[21] W. T. Ford,[21] J. F. Hirschauer,[21] A. Kreisel,[21] U. Nauenberg,[21] A. Olivas,[21] W. O. Ruddick,[21] J. G. Smith,[21] K. A. Ulmer,[21] S. R. Wagner,[21] J. Zhang,[21] A. Chen,[22] E. A. Eckhart,[22] A. Soffer,[22] W. H. Toki,[22] R. J. Wilson,[22] Q. Zeng,[22] D. Altenburg,[23] E. Feltresi,[23] A. Hauke,[23] B. Spaan,[23] T. Brandt,[24] J. Brose,[24] M. Dickopp,[24] V. Klose,[24] H. M. Lacker,[24] R. Nogowski,[24] S. Otto,[24] A. Petzold,[24] J. Schubert,[24] K. R. Schubert,[24] R. Schwierz,[24] J. E. Sundermann,[24] D. Bernard,[25] G. R. Bonneaud,[25] P. Grenier,[25] S. Schrenk,[25] Ch. Thiebaux,[25] G. Vasileiadis,[25] M. Verderi,[25] D. J. Bard,[26] P. J. Clark,[26] W. Gradl,[26] F. Muheim,[26] S. Playfer,[26] Y. Xie,[26] M. Andreotti,[27] V. Azzolini,[27] D. Bettoni,[27] C. Bozzi,[27] R. Calabrese,[27] G. Cibinetto,[27] E. Luppi,[27] M. Negrini,[27] L. Piemontese,[27] F. Anulli,[28] R. Baldini-Ferroli,[28] A. Calcaterra,[28] R. de Sangro,[28] G. Finocchiaro,[28] P. Patteri,[28] I. M. Peruzzi,[28,*] M. Piccolo,[28] A. Zallo,[28] A. Buzzo,[29] R. Capra,[29] R. Contri,[29] M. Lo Vetere,[29] M. Macri,[29] M. R. Monge,[29] S. Passaggio,[29] C. Patrignani,[29] E. Robutti,[29] A. Santroni,[29] S. Tosi,[29] G. Brandenburg,[30] K. S. Chaisanguanthum,[30] M. Morii,[30] E. Won,[30] J. Wu,[30] R. S. Dubitzky,[31] U. Langenegger,[31] J. Marks,[31] S. Schenk,[31] U. Uwer,[31] G. Schott,[32] W. Bhimji,[33] D. A. Bowerman,[33] P. D. Dauncey,[33] U. Egede,[33] R. L. Flack,[33] J. R. Gaillard,[33] J. A. Nash,[33] M. B. Nikolich,[33] W. Panduro Vazquez,[33] X. Chai,[34] M. J. Charles,[34] W. F. Mader,[34] U. Mallik,[34] A. K. Mohapatra,[34] V. Ziegler,[34] J. Cochran,[35] H. B. Crawley,[35] V. Eyges,[35] W. T. Meyer,[35] S. Prell,[35] E. I. Rosenberg,[35] A. E. Rubin,[35] J. Yi,[35] N. Arnaud,[36] M. Davier,[36] X. Giroux,[36] G. Grosdidier,[36] A. Höcker,[36] F. Le Diberder,[36] V. Lepeltier,[36] A. M. Lutz,[36] A. Oyanguren,[36] T. C. Petersen,[36] S. Plaszczynski,[36] S. Rodier,[36] P. Roudeau,[36] M. H. Schune,[36] A. Stocchi,[36] G. Wormser,[36] C. H. Cheng,[37] D. J. Lange,[37] M. C. Simani,[37] D. M. Wright,[37] A. J. Bevan,[38] C. A. Chavez,[38] I. J. Forster,[38] J. R. Fry,[38] E. Gabathuler,[38] R. Gamet,[38] K. A. George,[38] D. E. Hutchcroft,[38] R. J. Parry,[38] D. J. Payne,[38] K. C. Schofield,[38] C. Touramanis,[38] C. M. Cormack,[39] F. Di Lodovico,[39] W. Menges,[39] R. Sacco,[39] C. L. Brown,[40] G. Cowan,[40] H. U. Flaecher,[40] M. G. Green,[40] D. A. Hopkins,[40] P. S. Jackson,[40] T. R. McMahon,[40] S. Ricciardi,[40] F. Salvatore,[40] D. Brown,[41] C. L. Davis,[41] J. Allison,[42] N. R. Barlow,[42] R. J. Barlow,[42] C. L. Edgar,[42] M. C. Hodgkinson,[42] M. P. Kelly,[42] G. D. Lafferty,[42] M. T. Naisbit,[42] J. C. Williams,[42] C. Chen,[43] W. D. Hulsbergen,[43] A. Jawahery,[43]

D. Kovalskyi,[43] C. K. Lae,[43] D. A. Roberts,[43] G. Simi,[43] G. Blaylock,[44] C. Dallapiccola,[44] S. S. Hertzbach,[44] R. Kofler,[44] V. B. Koptchev,[44] X. Li,[44] T. B. Moore,[44] S. Saremi,[44] H. Staengle,[44] S. Willocq,[44] R. Cowan,[45] K. Koeneke,[45] G. Sciolla,[45] S. J. Sekula,[45] M. Spitznagel,[45] F. Taylor,[45] R. K. Yamamoto,[45] H. Kim,[46] P. M. Patel,[46] S. H. Robertson,[46] A. Lazzaro,[47] V. Lombardo,[47] F. Palombo,[47] J. M. Bauer,[48] L. Cremaldi,[48] V. Eschenburg,[48] R. Godang,[48] R. Kroeger,[48] J. Reidy,[48] D. A. Sanders,[48] D. J. Summers,[48] H. W. Zhao,[48] S. Brunet,[49] D. Côté,[49] P. Taras,[49] B. Viaud,[49] H. Nicholson,[50] N. Cavallo,[51,†] G. De Nardo,[51] F. Fabozzi,[51,†] C. Gatto,[51] L. Lista,[51] D. Monorchio,[51] P. Paolucci,[51] D. Piccolo,[51] C. Sciacca,[51] M. Baak,[52] H. Bulten,[52] G. Raven,[52] H. L. Snoek,[52] L. Wilden,[52] C. P. Jessop,[53] J. M. LoSecco,[53] T. Allmendinger,[54] G. Benelli,[54] K. K. Gan,[54] K. Honscheid,[54] D. Hufnagel,[54] P. D. Jackson,[54] H. Kagan,[54] R. Kass,[54] T. Pulliam,[54] A. M. Rahimi,[54] R. Ter-Antonyan,[54] Q. K. Wong,[54] J. Brau,[55] R. Frey,[55] O. Igonkina,[55] M. Lu,[55] C. T. Potter,[55] N. B. Sinev,[55] D. Strom,[55] J. Strube,[55] E. Torrence,[55] F. Galeazzi,[56] M. Margoni,[56] M. Morandin,[56] M. Posocco,[56] M. Rotondo,[56] F. Simonetto,[56] R. Stroili,[56] C. Voci,[56] M. Benayoun,[57] H. Briand,[57] J. Chauveau,[57] P. David,[57] L. Del Buono,[57] Ch. de la Vaissière,[57] O. Hamon,[57] M. J. J. John,[57] Ph. Leruste,[57] J. Malclès,[57] J. Ocariz,[57] L. Roos,[57] G. Therin,[57] P. K. Behera,[58] L. Gladney,[58] Q. H. Guo,[58] J. Panetta,[58] M. Biasini,[59] R. Covarelli,[59] S. Pacetti,[59] M. Pioppi,[59] C. Angelini,[60] G. Batignani,[60] S. Bettarini,[60] F. Bucci,[60] G. Calderini,[60] M. Carpinelli,[60] R. Cenci,[60] F. Forti,[60] M. A. Giorgi,[60] A. Lusiani,[60] G. Marchiori,[60] M. Morganti,[60] N. Neri,[60] E. Paoloni,[60] M. Rama,[60] G. Rizzo,[60] J. Walsh,[60] M. Haire,[61] D. Judd,[61] D. E. Wagoner,[61] J. Biesiada,[62] N. Danielson,[62] P. Elmer,[62] Y. P. Lau,[62] C. Lu,[62] J. Olsen,[62] A. J. S. Smith,[62] A. V. Telnov,[62] F. Bellini,[63] G. Cavoto,[63] A. D'Orazio,[63] E. Di Marco,[63] R. Faccini,[63] F. Ferrarotto,[63] F. Ferroni,[63] M. Gaspero,[63] L. Li Gioi,[63] M. A. Mazzoni,[63] S. Morganti,[63] G. Piredda,[63] F. Polci,[63] F. Safai Tehrani,[63] C. Voena,[63] H. Schröder,[64] G. Wagner,[64] R. Waldi,[64] T. Adye,[65] N. De Groot,[65] B. Franek,[65] G. P. Gopal,[65] E. O. Olaiya,[65] F. F. Wilson,[65] R. Aleksan,[66] S. Emery,[66] A. Gaidot,[66] S. F. Ganzhur,[66] G. Graziani,[66] G. Hamel de Monchenault,[66] W. Kozanecki,[66] M. Legendre,[66] G. W. London,[66] B. Mayer,[66] G. Vasseur,[66] Ch. Yèche,[66] M. Zito,[66] M. V. Purohit,[67] A. W. Weidemann,[67] J. R. Wilson,[67] F. X. Yumiceva,[67] T. Abe,[68] M. T. Allen,[68] D. Aston,[68] R. Bartoldus,[68] N. Berger,[68] A. M. Boyarski,[68] O. L. Buchmueller,[68] R. Claus,[68] J. P. Coleman,[68] M. R. Convery,[68] M. Cristinziani,[68] J. C. Dingfelder,[68] D. Dong,[68] J. Dorfan,[68] D. Dujmic,[68] W. Dunwoodie,[68] S. Fan,[68] R. C. Field,[68] T. Glanzman,[68] S. J. Gowdy,[68] T. Hadig,[68] V. Halyo,[68] C. Hast,[68] T. Hryn'ova,[68] W. R. Innes,[68] M. H. Kelsey,[68] P. Kim,[68] M. L. Kocian,[68] D. W. G. S. Leith,[68] J. Libby,[68] S. Luitz,[68] V. Luth,[68] H. L. Lynch,[68] H. Marsiske,[68] R. Messner,[68] D. R. Muller,[68] C. P. O'Grady,[68] V. E. Ozcan,[68] A. Perazzo,[68] M. Perl,[68] B. N. Ratcliff,[68] A. Roodman,[68] A. A. Salnikov,[68] R. H. Schindler,[68] J. Schwiening,[68] A. Snyder,[68] J. Stelzer,[68] D. Su,[68] M. K. Sullivan,[68] K. Suzuki,[68] S. K. Swain,[68] J. M. Thompson,[68] J. Va'vra,[68] N. van Bakel,[68] M. Weaver,[68] W. J. Wisniewski,[68] M. Wittgen,[68] D. H. Wright,[68] A. K. Yarritu,[68] K. Yi,[68] C. C. Young,[68] P. R. Burchat,[69] A. J. Edwards,[69] S. A. Majewski,[69] B. A. Petersen,[69] C. Roat,[69] M. Ahmed,[70] S. Ahmed,[70] M. S. Alam,[70] R. Bula,[70] J. A. Ernst,[70] M. A. Saeed,[70] F. R. Wappler,[70] S. B. Zain,[70] W. Bugg,[71] M. Krishnamurthy,[71] S. M. Spanier,[71] R. Eckmann,[72] J. L. Ritchie,[72] A. Satpathy,[72] R. F. Schwitters,[72] J. M. Izen,[73] I. Kitayama,[73] X. C. Lou,[73] S. Ye,[73] F. Bianchi,[74] M. Bona,[74] F. Gallo,[74] D. Gamba,[74] M. Bomben,[75] L. Bosisio,[75] C. Cartaro,[75] F. Cossutti,[75] G. Della Ricca,[75] S. Dittongo,[75] S. Grancagnolo,[75] L. Lanceri,[75] L. Vitale,[75] F. Martinez-Vidal,[76] R. S. Panvini,[77,‡] Sw. Banerjee,[78] B. Bhuyan,[78] C. M. Brown,[78] D. Fortin,[78] K. Hamano,[78] R. Kowalewski,[78] J. M. Roney,[78] R. J. Sobie,[78] J. J. Back,[79] P. F. Harrison,[79] T. E. Latham,[79] G. B. Mohanty,[79] H. R. Band,[80] X. Chen,[80] B. Cheng,[80] S. Dasu,[80] M. Datta,[80] A. M. Eichenbaum,[80] K. T. Flood,[80] M. Graham,[80] J. J. Hollar,[80] J. R. Johnson,[80] P. E. Kutter,[80] H. Li,[80] R. Liu,[80] B. Mellado,[80] A. Mihalyi,[80] Y. Pan,[80] M. Pierini,[80] R. Prepost,[80] P. Tan,[80] S. L. Wu,[80] Z. Yu,[80] and H. Neal[81]

(The *BABAR* Collaboration)

[1]*Laboratoire de Physique des Particules, F-74941 Annecy-le-Vieux, France*
[2]*IFAE, Universitat Autonoma de Barcelona, E-08193 Bellaterra, Barcelona, Spain*
[3]*Università di Bari, Dipartimento di Fisica and INFN, I-70126 Bari, Italy*
[4]*Institute of High Energy Physics, Beijing 100039, China*
[5]*University of Bergen, Inst. of Physics, N-5007 Bergen, Norway*
[6]*Lawrence Berkeley National Laboratory and University of California, Berkeley, California 94720, USA*
[7]*University of Birmingham, Birmingham, B15 2TT, United Kingdom*
[8]*Ruhr Universität Bochum, Institut für Experimentalphysik 1, D-44780 Bochum, Germany*
[9]*University of Bristol, Bristol BS8 1TL, United Kingdom*
[10]*University of British Columbia, Vancouver, British Columbia, Canada V6T 1Z1*
[11]*Brunel University, Uxbridge, Middlesex UB8 3PH, United Kingdom*

[12]Budker Institute of Nuclear Physics, Novosibirsk 630090, Russia
[13]University of California at Irvine, Irvine, California 92697, USA
[14]University of California at Los Angeles, Los Angeles, California 90024, USA
[15]University of California at Riverside, Riverside, California 92521, USA
[16]University of California at San Diego, La Jolla, California 92093, USA
[17]University of California at Santa Barbara, Santa Barbara, California 93106, USA
[18]University of California at Santa Cruz, Institute for Particle Physics, Santa Cruz, California 95064, USA
[19]California Institute of Technology, Pasadena, California 91125, USA
[20]University of Cincinnati, Cincinnati, Ohio 45221, USA
[21]University of Colorado, Boulder, Colorado 80309, USA
[22]Colorado State University, Fort Collins, Colorado 80523, USA
[23]Universität Dortmund, Institut für Physik, D-44221 Dortmund, Germany
[24]Technische Universität Dresden, Institut für Kern- und Teilchenphysik, D-01062 Dresden, Germany
[25]Ecole Polytechnique, LLR, F-91128 Palaiseau, France
[26]University of Edinburgh, Edinburgh EH9 3JZ, United Kingdom
[27]Università di Ferrara, Dipartimento di Fisica and INFN, I-44100 Ferrara, Italy
[28]Laboratori Nazionali di Frascati dell'INFN, I-00044 Frascati, Italy
[29]Università di Genova, Dipartimento di Fisica and INFN, I-16146 Genova, Italy
[30]Harvard University, Cambridge, Massachusetts 02138, USA
[31]Universität Heidelberg, Physikalisches Institut, Philosophenweg 12, D-69120 Heidelberg, Germany
[32]Universität Karlsruhe, Institut für Experimentelle Kernphysik, D-76021 Karlsruhe, Germany
[33]Imperial College London, London, SW7 2AZ, United Kingdom
[34]University of Iowa, Iowa City, Iowa 52242, USA
[35]Iowa State University, Ames, Iowa 50011-3160, USA
[36]Laboratoire de l'Accélérateur Linéaire, F-91898 Orsay, France
[37]Lawrence Livermore National Laboratory, Livermore, California 94550, USA
[38]University of Liverpool, Liverpool L69 72E, United Kingdom
[39]Queen Mary, University of London, E1 4NS, United Kingdom
[40]University of London, Royal Holloway and Bedford New College, Egham, Surrey TW20 0EX, United Kingdom
[41]University of Louisville, Louisville, Kentucky 40292, USA
[42]University of Manchester, Manchester M13 9PL, United Kingdom
[43]University of Maryland, College Park, Maryland 20742, USA
[44]University of Massachusetts, Amherst, Massachusetts 01003, USA
[45]Massachusetts Institute of Technology, Laboratory for Nuclear Science, Cambridge, Massachusetts 02139, USA
[46]McGill University, Montréal, Quebec, Canada H3A 2T8
[47]Università di Milano, Dipartimento di Fisica and INFN, I-20133 Milano, Italy
[48]University of Mississippi, University, Mississippi 38677, USA
[49]Université de Montréal, Laboratoire René J. A. Lévesque, Montréal, Quebec, Canada H3C 3J7
[50]Mount Holyoke College, South Hadley, Massachusetts 01075, USA
[51]Università di Napoli Federico II, Dipartimento di Scienze Fisiche and INFN, I-80126, Napoli, Italy
[52]NIKHEF, National Institute for Nuclear Physics and High Energy Physics, NL-1009 DB Amsterdam, The Netherlands
[53]University of Notre Dame, Notre Dame, Indiana 46556, USA
[54]Ohio State University, Columbus, Ohio 43210, USA
[55]University of Oregon, Eugene, Oregon 97403, USA
[56]Università di Padova, Dipartimento di Fisica and INFN, I-35131 Padova, Italy
[57]Universités Paris VI et VII, Laboratoire de Physique Nucléaire et de Hautes Energies, F-75252 Paris, France
[58]University of Pennsylvania, Philadelphia, Pennsylvania 19104, USA
[59]Università di Perugia, Dipartimento di Fisica and INFN, I-06100 Perugia, Italy
[60]Università di Pisa, Dipartimento di Fisica, Scuola Normale Superiore and INFN, I-56127 Pisa, Italy
[61]Prairie View A&M University, Prairie View, Texas 77446, USA
[62]Princeton University, Princeton, New Jersey 08544, USA
[63]Università di Roma La Sapienza, Dipartimento di Fisica and INFN, I-00185 Roma, Italy
[64]Universität Rostock, D-18051 Rostock, Germany
[65]Rutherford Appleton Laboratory, Chilton, Didcot, Oxon, OX11 0QX, United Kingdom
[66]DSM/Dapnia, CEA/Saclay, F-91191 Gif-sur-Yvette, France
[67]University of South Carolina, Columbia, South Carolina 29208, USA
[68]Stanford Linear Accelerator Center, Stanford, California 94309, USA
[69]Stanford University, Stanford, California 94305-4060, USA
[70]State University of New York, Albany, New York 12222, USA
[71]University of Tennessee, Knoxville, Tennessee 37996, USA
[72]University of Texas at Austin, Austin, Texas 78712, USA
[73]University of Texas at Dallas, Richardson, Texas 75083, USA
[74]Università di Torino, Dipartimento di Fisica Sperimentale and INFN, I-10125 Torino, Italy
[75]Università di Trieste, Dipartimento di Fisica and INFN, I-34127 Trieste, Italy

[76] IFIC, Universitat de Valencia-CSIC, E-46071 Valencia, Spain
[77] Vanderbilt University, Nashville, Tennessee 37235, USA
[78] University of Victoria, Victoria, British Columbia, Canada V8W 3P6
[79] Department of Physics, University of Warwick, Coventry CV4 7AL, United Kingdom
[80] University of Wisconsin, Madison, Wisconsin 53706, USA
[81] Yale University, New Haven, Connecticut 06511, USA

(Dated: February 5, 2008)

A search for the non-conservation of lepton flavor in the decay $\tau^{\pm} \rightarrow e^{\pm}\gamma$ has been performed with 2.07×10^{8} $e^+e^- \rightarrow \tau^+\tau^-$ events collected by the *BABAR* detector at the PEP-II storage ring at a center-of-mass energy near 10.58 GeV. We find no evidence for a signal and set an upper limit on the branching ratio of $\mathcal{B}(\tau^{\pm} \rightarrow e^{\pm}\gamma) < 1.1 \times 10^{-7}$ at 90% confidence level.

PACS numbers: 13.35.Dx, 11.30.Hv, 14.60.Fg

Lepton flavor conservation differs from other conservation laws in the Standard Model (SM) because it is not associated with an underlying conserved current symmetry. Consequently, new theories attempting to describe nature beyond the SM often include lepton flavor violating processes such as the neutrino-less decay of a μ or τ lepton, which have long been identified as unambiguous signatures of new physics. If no specific theoretical model is assumed, any or all of the $\mu \rightarrow e\gamma$, $\tau \rightarrow \mu\gamma$ and $\tau \rightarrow e\gamma$ decays can be expected to be observed, and therefore independent searches for each of these modes are required. Some theoretical models [1, 2] respecting the current limits on $\mathcal{B}(\mu^+ \rightarrow e^+\gamma)$ [3] and $\mathcal{B}(\tau^{\pm} \rightarrow \mu^{\pm}\gamma)$ [4] in fact allow $\tau^{\pm} \rightarrow e^{\pm}\gamma$ decays to occur up to the existing experimental bound [5].

A significant improvement on this $\tau^{\pm} \rightarrow e^{\pm}\gamma$ limit is presented here using data recorded by the *BABAR* detector at the SLAC PEP-II asymmetric-energy e^+e^- storage ring. The data sample consists of an integrated luminosity of Ł= 210.6 fb^{-1} recorded at a center-of-mass (c.m.) energy ($\sqrt{s}$) of $\sqrt{s} = 10.58$ GeV, and 21.6 fb^{-1} recorded at $\sqrt{s} = 10.54$ GeV. With an average cross section of $\sigma_{e^+e^- \rightarrow \tau^+\tau^-} = (0.89 \pm 0.02)$ nb [6] as determined using the `KK2F` Monte Carlo (MC) generator [7], this corresponds to a data sample of 2.07×10^{8} τ-pair events.

The *BABAR* detector is described in detail in Ref. [8]. Charged particles are reconstructed as tracks with a 5-layer silicon vertex tracker and a 40-layer drift chamber (DCH) inside a 1.5 T solenoidal magnet. An electromagnetic calorimeter (EMC) consisting of 6580 CsI(Tl) crystals is used to identify electrons and photons. A ring-imaging Cherenkov detector (DIRC) is used to identify charged hadrons and provides additional electron identification information.

The signature of the signal process is the presence of an isolated $e\gamma$ pair having an invariant mass consistent with that of the τ (1.777 GeV/c^2 [9]) and a total energy ($E_{e\gamma}$) equal to $\sqrt{s}/2$ in the c.m. frame, along with other particles in the event with properties consistent with a SM τ decay. Such events are simulated with higher-order radiative corrections using the `KK2F` MC generator [7] where one τ decays into $e\gamma$ according to phase space [10], while the other τ decays according to measured branching ratios [11] simulated with the `TAUOLA` MC generator [12, 13]. The detector response is simulated with the `GEANT4` package [14]. The simulated events for signal as well as SM background processes [7, 12, 13, 15, 16, 17] are then reconstructed in the same manner as data. The MC backgrounds are used to optimize the selection criteria and study systematic errors in the efficiency estimates, but not for the estimation of the final background rate, which relies solely on data. For the background from Bhabha events, we do not rely upon MC predictions because the large Bhabha cross section makes generation of a sufficiently large MC sample impractical.

Events with zero total charge and with two or four well-reconstructed tracks inconsistent with coming from a photon conversion are selected. The event is divided into hemispheres by the plane perpendicular to the thrust axis. The thrust axis, which characterizes the direction of maximum energy flow in the c.m. frame of the event [18], is calculated using all observed charged and neutral particles.

The signal-side hemisphere is required to contain at least one γ with a c.m. energy greater than 500 MeV, and one track identified as an electron. The electron identification uses DCH, EMC and DIRC information, including a requirement that the E/p ratio (the energy deposited in the EMC by the charged particle divided by its momentum as measured in the DCH) lies between 0.89 and 1.2. The electron candidate is required to lie within the fiducial acceptance of the EMC and to have a momentum greater than 500 MeV/c. These criteria yield a π misidentification rate of less than 0.3%. The efficiency for correctly identifying reconstructed tracks in the fiducial volume as electrons in $\tau^{\pm} \rightarrow e^{\pm}\gamma$ MC events is greater than 91%. For events with more than one signal-side γ candidate, we choose the γ which gives the mass of the $e\gamma$ system closest to the τ mass. This provides the correct pairing for 99.9% of selected signal MC events.

The resolution of the $e\gamma$ mass is improved by assigning the point of closest approach of the e track to the e^+e^- collision axis as the origin of the γ candidate and by using a kinematic fit with $E_{e\gamma}$ constrained to

$\sqrt{s}/2$. The resulting energy-constrained mass ($m_{\rm EC}$) and $\Delta E = E_{e\gamma} - \sqrt{s}/2$ are independent variables apart from small correlations arising from initial and final state radiation. The mean and standard deviation of the $m_{\rm EC}$ and ΔE distributions for reconstructed MC signal events are: $\langle m_{\rm EC}\rangle = 1777\,{\rm MeV}/c^2$, $\sigma(m_{\rm EC}) = 9\,{\rm MeV}/c^2$, $\langle \Delta E\rangle = -15\,{\rm MeV}$, $\sigma(\Delta E) = 51\,{\rm MeV}$, where the shift in $\langle \Delta E\rangle$ comes from photon energy reconstruction effects. To minimize possible biases, we perform a blind analysis by excluding all events in the data within a $\pm 3\sigma$ rectangular box centered on $\langle m_{\rm EC}\rangle$ and $\langle \Delta E\rangle$ until all optimization and systematic studies of the selection criteria have been completed. We optimize the selection to obtain the smallest expected upper limit in a background-only hypothesis for observing events inside a $\pm 2\sigma$ rectangular box signal box defined by: $|\Delta E - \langle \Delta E\rangle| < 2\sigma(\Delta E)$ and $|m_{\rm EC} - m_\tau| < 2\sigma(m_{\rm EC})$, as shown in Figure 1.

The dominant backgrounds arise from Bhabha and $e^+e^- \to \tau^+\tau^-$ (with a $\tau \to e\nu\overline{\nu}$ decay) processes with an energetic γ from initial or final state radiation or from $\tau \to e\nu\overline{\nu}\gamma$ decays. Backgrounds arising from radiation are reduced by requiring that the total c.m. energy of all non-signal γ candidates in the signal-side hemisphere be less than 200 MeV. To suppress non-τ backgrounds with significant radiation along the beam directions, the polar angle (θ_{miss}) of the missing momentum associated with the neutrino(s) in the event is required to lie within the detector acceptance ($-0.76 < \cos\theta_{miss} < 0.92$).

The tag-side hemisphere, defined to be that opposite to the signal-side hemisphere, is expected to contain a SM τ decay characterized by the presence of one or three charged particles and missing momentum due to unobserved neutrino(s). Taking the direction of the tag-side τ to be opposite the signal $e\gamma$ candidate, we use all tracks and γ candidates in the tag-side hemisphere to calculate the invariant mass squared of the tag-side missing momentum (m^2_ν), which peaks around zero for the signal. To reduce backgrounds from radiative $e^+e^- \to \tau^+\tau^-$ processes, we require $m^2_\nu > -0.25\ {\rm GeV}^2/c^4$.

The component of the missing momentum of the event transverse to the collision axis scaled to the beam energy ($2 \times p^T_{miss}/\sqrt{s}$) is expected to be large for signal and $e^+e^- \to \tau^+\tau^-$ events, but small for Bhabha and 2-photon events. We exploit an observed correlation between m^2_ν and ($2 \times p^T_{miss}/\sqrt{s}$) in the non-$\tau$ backgrounds to significantly suppress them. We require the following: $(m^2_\nu/1.8\,{\rm GeV}^2/c^4) - \ln(2 \times p^T_{miss}/\sqrt{s})/2.0 < 1$, the highest c.m. momentum track on the tag-side hemisphere to be inconsistent with being an electron, including requirements that E/p be less than 0.5 and that the momentum be greater than $500\,{\rm MeV}/c$, and the tag-side hemisphere to have a total c.m. momentum of all charged and neutral particles less than $4.75\,{\rm GeV}/c$.

Backgrounds from $e^+e^- \to q\overline{q}$ processes are further reduced by requiring the total invariant mass of particles in the tag-side hemisphere to be less than $1.8\,{\rm GeV}/c^2$.

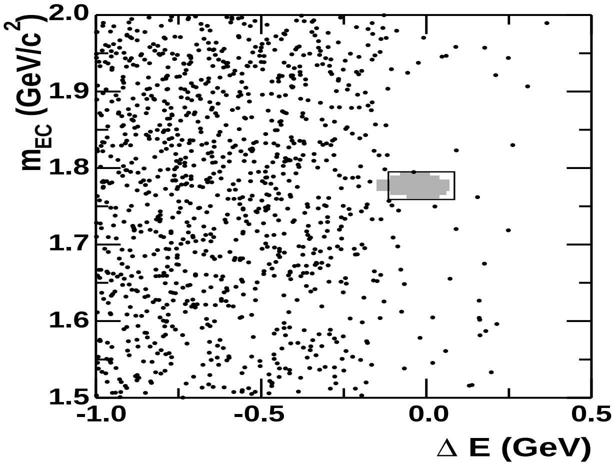

FIG. 1: $m_{\rm EC}$ vs. ΔE distribution of data (dots) and shaded region containing 50% of the selected signal MC events inside the Grand Signal Box, as defined in the text. The boundary of the $\pm 2\sigma$ signal box is also shown.

After this selection, 8.9% of the total generated MC signal events survive within a Grand Signal Box (GSB) region defined as follows: $m_{\rm EC} \in [1.5, 2.0]$ GeV/c^2, $\Delta E \in [-1.0, 0.5]$ GeV. The data distribution of $m_{\rm EC}$ and ΔE inside the GSB is plotted as dots in Figure 1, along with a shaded region containing 50% of the selected signal MC events shown for illustrative purposes. The GSB excluding the $\pm 3\sigma$ blind region contains 1110 data events, while the luminosity-normalized sum of the non-Bhabha MC backgrounds yield 1045 events. Of these MC events, 99.8% are $e^+e^- \to \tau^+\tau^-$ events, 99.9% of which have $\tau \to e\nu\overline{\nu}$ decays on the signal-side.

The (5.9 ± 3.7)% difference between the number of data and τ-pair dominated MC events indicates that the Bhabha background level in the GSB is low. However, in the more restrictive $|\Delta E - \langle \Delta E\rangle| < 2\sigma(\Delta E)$ region, the Bhabha background is expected to contribute a substantially higher background fraction because of the greater likelihood of a Bhabha than a τ-pair event to have a hemisphere containing the full beam energy. This residual Bhabha contamination is studied using data distributions of the deviation (ΔE_γ) of the measured photon c.m. energy from the corresponding prediction assuming a fully contained $e^+e^- \to e^+e^-\gamma$ event. The predicted photon energy is obtained from the beam energy and kinematic information from all particles in the event except the measured photon energy. We observe that the excess of data over non-Bhabha MC events is clustered at low ΔE_γ, where the Bhabha events are expected to appear. As we progressively loosen the electron veto on the tag-side track, the excess in the number of data events over the non-Bhabha MC background grows in the region with small ΔE_γ, providing further confirmation that the Bhabha background is well understood.

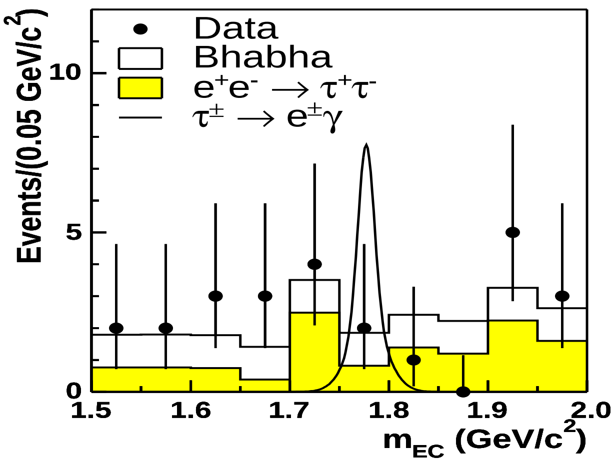

FIG. 2: $m_{\rm EC}$ distribution of data (dots), the expected backgrounds (histograms) and MC signal (curve with arbitrary normalization) for $|\Delta E - \langle \Delta E \rangle| < 2\sigma(\Delta E)$.

We cross check the Bhabha contamination in the $|\Delta E - \langle \Delta E \rangle| < 2\sigma(\Delta E)$ region from a data sample without a tag-side electron veto, by removing the E/p requirement on the tag-side. To estimate the Bhabha contamination surviving our final event selection, which includes a cut of tag-side $E/p < 0.5$, we use the data in the adjacent Bhabha-dominated E/p region, $0.5 < E/p < 1.2$. We extrapolate the rate from the $0.5 < E/p < 1.2$ region to the $E/p < 0.5$ region, using a high statistics and high purity Bhabha control sample obtained by reversing the requirement on $(m_\nu^2/1.8\,{\rm GeV}^2/c^4) - \ln(2 \times p^T_{miss}/\sqrt{s})/2.0$ given above. We estimate the residual Bhabha contamination in our final selection by multiplying the number of events in the $0.5 < E/p < 1.2$ region of the no tag-side electron veto sample by the ratio of the number of events in the Bhabha control sample in the $E/p < 0.5$ region to that in the $0.5 < E/p < 1.2$ region. This method gives an estimate of 10.3±1.1 Bhabha events inside the $\pm 2\sigma(\Delta E)$ band once the tag-side electron veto is applied.

In this band, we expect 12.9±2.5 events from the non-Bhabha MC backgrounds, thus obtaining a total background estimate of 23.2±2.7 events. This compares well with the 25 events observed inside the $\pm 2\sigma(\Delta E)$ band in the data. We also find good agreement between the observed and expected number of events separately for the sub-samples with one and three tracks on the tag-side.

For the final background estimate we use the $m_{\rm EC}$ distribution of data events inside the $\pm 2\sigma(\Delta E)$ band, as shown in Figure 2 along with the signal shape included for illustrative purposes. The backgrounds from data inside the $\pm 2\sigma(\Delta E)$ band with $|m_{\rm EC} - m_\tau| > 3\sigma(m_{\rm EC})$ are fitted to different orders of polynomials in $m_{\rm EC}$ using a maximum likelihood approach. A fit with a constant probability density function (PDF) yields a total χ^2 of 4.7 for the 10 bins shown in Figure 2, and predicts 1.9±0.4 events inside the final $\pm 2\sigma(m_{\rm EC})$ signal region. Equally acceptable goodness of fit is obtained with higher-order polynomials. However, the coefficients of the higher order terms are statistically compatible with zero. The background predictions from these PDFs agree with the prediction from the constant PDF to within ±0.3 events. As these deviations are smaller than the statistical error on the prediction from the constant PDF, we conclude that the data $m_{\rm EC}$ distribution is consistent with being uniform.

A cross check using non-Bhabha MC background contributions combined with residual Bhabha contamination estimates obtained from the data is also found to be reasonably uniform in $m_{\rm EC}$ (Figure 2) and predicts 1.7±0.2 events inside the $\pm 2\sigma(m_{\rm EC})$ signal box.

The (5.9±3.7)% difference between data and τ-pair MC predictions also provides a measure of our ability to model the signal-like events in the GSB, since these data events have very similar characteristics to the signal, both in terms of the trigger response of the experiment as well as for the distributions of all the selection variables apart from $m_{\rm EC}$ and ΔE. The systematic error due to a particular cut is taken as the product of the marginal efficiency of the cut and the relative discrepancy between data and MC in the GSB after all other cuts have been applied. The contributions from all the different cuts added in quadrature yield a 2.3% relative systematic error, the only appreciable effect being associated with the requirements on m_ν^2 and $p^T_{\rm miss}$. This approach yields a more conservative estimate of the systematic uncertainty on the signal efficiency than the more traditional approach derived from considering the difference between the data and MC prediction for each selection variable, which gives a total estimate of 2.0% relative contribution from all the cuts.

The relative systematic uncertainties on the trigger efficiency, tracking and photon reconstruction efficiencies, and particle identification are estimated to be 1.4%, 1.3%, 1.8% and 1.3%, respectively. The requirement that the events fall within the $\pm 2\sigma$ signal box in $m_{\rm EC}$ and ΔE contributes a 4.4% systematic error associated with the scale and resolution uncertainties of these variables and a small contribution from the beam energy uncertainty. As we use 1.3 million MC signal events, the contribution to the uncertainty arising from signal MC statistics is negligible. Adding the contributions of the individual terms in quadrature with an additional 2.3% normalization error on the product $Ł\sigma_{\tau\tau}$ gives a 6.2% total relative systematic uncertainty on $Ł\sigma_{\tau\tau}\varepsilon$ in the signal box, where the efficiency is $\varepsilon = (4.7 \pm 0.3)\%$. We note that our final limit on the branching ratio is insensitive to the systematic uncertainty as long as this uncertainty is below 10%.

We find one event in the signal box for an expected background of 1.9±0.4 events. Because of the low background levels, we do not fit for a signal in the $m_{\rm EC}$ distribution as is done in our recent search for $\tau^\pm \to \mu^\pm\gamma$

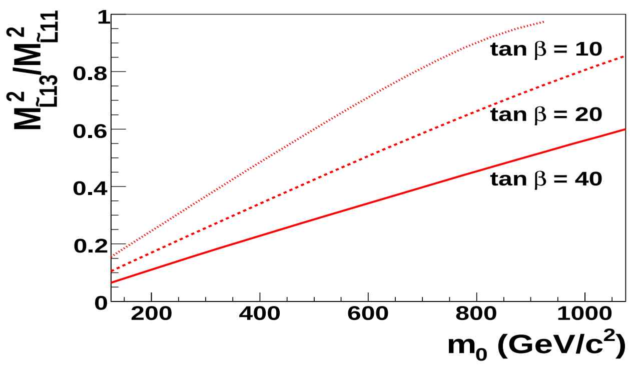

FIG. 3: 90% C.L. upper limits on $M^2_{\tilde{L}13}/M^2_{\tilde{L}11}$ for $\mathcal{B}(\tau^\pm \to e^\pm\gamma) < 1.1 \times 10^{-7}$ with $\tan\beta = 10$, 20 and 40.

[4]. Rather, we set an upper limit employing the same technique used in our search for $\tau^\pm \to \ell^\pm\ell^+\ell^-$ [19] where the background levels were also small. A 90% C.L. upper limit on the branching ratio is calculated according to $\mathcal{B}^{90}_{UL} = N^{90}_{UL}/(2\varepsilon\mathrm{L}\sigma_{\tau\tau})$, where N^{90}_{UL} is the 90% C.L. upper limit with one event observed when 1.9±0.4 events are expected. The limit is calculated including all uncertainties using the technique of Cousins and Highland [20] following the implementation of Barlow [21]. At 90% C.L. this procedure gives an upper limit of $\mathcal{B}(\tau^\pm \to e^\pm\gamma) < 1.1\times10^{-7}$ [22]. This represents a more than three-fold reduction in the upper limit as reported in [5].

As an example of how this result constrains theories beyond the SM, we set bounds on the ratio of the first and the third generation element to the first generation diagonal element ($M^2_{\tilde{L}13}/M^2_{\tilde{L}11}$) of the left-handed slepton mass matrix based on predictions from a minimal supergravity model [23, 24]. Figure 3 shows the upper limits on $M^2_{\tilde{L}13}/M^2_{\tilde{L}11}$ as a function of the ratio of the Higgs vacuum expectation values ($\tan\beta$) and the universal scalar mass (m_0), which, for simplicity, is set equal to the universal gaugino mass.

We are grateful for the excellent luminosity and machine conditions provided by our PEP-II colleagues, and for the substantial dedicated effort from the computing organizations that support *BABAR*. The collaborating institutions wish to thank SLAC for its support and kind hospitality. This work is supported by DOE and NSF (USA), NSERC (Canada), IHEP (China), CEA and CNRS-IN2P3 (France), BMBF and DFG (Germany), INFN (Italy), FOM (The Netherlands), NFR (Norway), MIST (Russia), and PPARC (United Kingdom). Individuals have received support from the A. P. Sloan Foundation, Research Corporation, and Alexander von Humboldt Foundation.

* Also with Università di Perugia, Dipartimento di Fisica, Perugia, Italy
† Also with Università della Basilicata, Potenza, Italy
‡ Deceased

[1] E. Ma, Nucl. Phys. Proc. Suppl. **123**, 125 (2003).
[2] J. R. Ellis, J. Hisano, M. Raidal and Y. Shimizu, Phys. Rev. D **66**, 115013 (2002).
[3] M. L. Brooks *et al.* (MEGA Collaboration), Phys. Rev. Lett. **83**, 1521 (1999). $\mathcal{B}(\mu^+ \to e^+\gamma) < 1.2 \times 10^{-11}$ at 90% C.L.
[4] B. Aubert *et al.* (*BABAR* Collaboration), Phys. Rev. Lett. **95**, 41802 (2005). $\mathcal{B}(\tau^\pm \to \mu^\pm\gamma) < 6.8\times10^{-8}$ at 90% C.L.
[5] K. Hayasaka *et al.* (Belle Collaboration), Phys. Lett. B **613**, 20 (2005). $\mathcal{B}(\tau^\pm \to e^\pm\gamma) < 3.9 \times 10^{-7}$ at 90% C.L.
[6] The uncertainty was conservatively estimated by comparing cross sections from `KK2F` [7] and `KORALB`: S. Jadach and Z. Was, Comput. Phys. Commun. **85**, 453 (1995).
[7] B. F. Ward, S. Jadach, and Z. Was, Nucl. Phys. Proc. Suppl. **116**, 73 (2003).
[8] B. Aubert *et al.* (*BABAR* Collaboration), Nucl. Instrum. Methods Phys. Res., Sect. A **479**, 1 (2002).
[9] J. Z. Bai *et al.* (BES Collaboration), Phys. Rev. D **53**, 20 (1996).
[10] Our limit is insensitive to the phase space assumption as cross-checked with the two extreme cases of a V − A and a V + A form of interaction for the signal MC.
[11] S. Eidelman *et al.* (Particle Data Group), Phys. Lett. B **592**, 1 (2004).
[12] S. Jadach, Z. Was, R. Decker, and J. H. Kuhn, Comput. Phys. Commun. **76**, 361 (1993).
[13] E. Barberio and Z. Was, Comput. Phys. Commun. **79**, 291 (1994).
[14] S. Agostinelli *et al.* (GEANT4 Collaboration), Nucl. Instrum. Methods Phys. Res., Sect. A **506**, 250 (2003).
[15] D. J. Lange, Nucl. Instrum. Methods Phys. Res., Sect. A **462**, 152 (2001).
[16] T. Sjöstrand, Comput. Phys. Commun. **82**, 74 (1994).
[17] S. Jadach, W. Placzek and B. F. L. Ward, Phys. Lett. B **390**, 298 (1997).
[18] S. Brandt *et al.*, Phys. Lett. **12** 57 (1964);
E. Fahri, Phys. Rev. Lett. **39** 1587 (1977).
[19] B. Aubert *et al.* (*BABAR* Collaboration), Phys. Rev. Lett. **92**, 121801 (2004).
[20] R. D. Cousins and V. L. Highland, Nucl. Instrum. Methods Phys. Res., Sect. A **320**, 331 (1992).
[21] R. Barlow, Comput. Phys. Commun. **149**, 97 (2002).
[22] For an equivalent toy MC experiment with no signal, the expected upper limit at 90% C.L. is $\mathcal{B}(\tau^\pm \to e^\pm\gamma) < 1.2 \times 10^{-7}$, similar to that obtained in Reference [4].
[23] A. Brignole and A. Rossi, Nucl. Phys. B **701**, 3 (2004).
[24] W. Porod, Comput. Phys. Commun. **153**, 275 (2003).

A search for the non-conservation of lepton flavor in the decay $\tau^{\pm} \rightarrow e^{\pm}\gamma$ has been performed with 2.07×10^{8} $e^{+}e^{-} \rightarrow \tau^{+}\tau^{-}$ events collected by the BABAR detector at the PEP-II storage ring at a center-of-mass energy near 10.58 GeV. We find no evidence for a signal and set an upper limit on the branching ratio of $\mathcal{B}(\tau^{\pm} \rightarrow e^{\pm}\gamma) < 1.1 \times 10^{-7}$ at 90% confidence level.